CORRELATIONS BETWEEN CHOROIDAL STRUCTURES AND VISUAL FUNCTIONS IN EYES WITH RETINITIS PIGMENTOSA

MARIKO EGAWA, MD, PhD,*† YOSHINORI MITAMURA, MD, PhD,*† MASANORI NIKI, MD,*†
HIROKI SANO, MD,*† GEN MIURA, MD, PhD,‡ AKIHIRO CHIBA, MD,‡
SHUICHI YAMAMOTO, MD, PhD,‡ SHOZO SONODA, MD, PhD,†§ TAIJI SAKAMOTO, MD, PhD†§

Purpose: To investigate the choroidal structures in the enhanced depth imaging optical coherence tomographic images in eyes with retinitis pigmentosa (RP) and to determine correlations between the choroidal structures and visual functions.

Methods: The enhanced depth imaging optical coherence tomographic images of 100 eyes with typical RP and 60 age-, sex-, and axial length–matched normal eyes were binarized using ImageJ. The cross-sectional luminal and stromal areas of the inner and outer subfoveal choroid of 1,500-μm width were measured. The inner choroid included the choriocapillaris and medium vessel layer, and the outer choroid included the larger vessel layer.

Results: In the inner choroid, the luminal area and the ratio of luminal/total choroidal area (L/C ratio) were significantly smaller in RP than in controls ($P = 0.010$, $P < 0.001$, respectively), whereas the stromal area was not significantly different ($P = 0.114$). The inner choroidal L/C ratio was significantly correlated with the best-corrected visual acuity, mean deviation, foveal sensitivity, width of the ellipsoid zone, and central foveal thickness in RP after adjusting for the axial length, age, and sex (all $P < 0.005$).

Conclusion: The significant correlations between the inner choroidal structures and the visual functions and retinal structures indicate that the choroidal structures are altered in association with the progression of RP.

RETINA 39:2399–2409, 2019

Retinitis pigmentosa (RP) is a heterogeneous group of hereditary, retinal, degenerative diseases characterized by night blindness, progressive concentric visual field loss, and eventual loss of central vision.[1] The primary lesion in RP is the apoptosis of the rod photoreceptors followed by a progressive and irreversible death of the cones.[2] The degeneration of the rods is due to a mutation of a gene associated with a protein of the rods.

A decrease in the choroidal blood flow has also been reported in patients with RP.[3–5] In a rat model of retinal degeneration, the delayed death of the cone cells after light toxicity has been attributed to a decrease in choroidal circulation.[6] It was reported that the increase in the plasma level of endothelin-1, a powerful vasoconstrictor of small and large blood vessels, was related to the decrease in foveal choroidal blood flow in patients with RP.[7] The results of earlier studies on animal models of RP demonstrated a loss of the capillaries in the choroid.[8,9] Fluorescein angiography demonstrated pathologic changes in the choroidal vessel in eyes of patients with RP.[10] Thus, it has been suggested that improving the choroidal circulation

might preserve the cone photoreceptors in patients with RP.[6,11] However, the relationships between these choroidal changes and progression of RP have not been determined.

Earlier studies using enhanced depth imaging optical coherence tomography (EDI-OCT) showed that the subfoveal choroid was significantly thinner in eyes with RP.[12,13] We have reported that the EDI-OCT images can be converted to binary images, which can then be used to quantify the luminal and stromal areas of the choroid separately.[14–18] This technique has been widely used to investigate the choroidal structures.[14–19] Most recently, Kawano et al[20] compared the structural changes in the whole choroid in the areas with greater retinal degeneration to the areas with less retinal degeneration in eyes with RP. The results showed that the cross-sectional area of the whole choroid was smaller beneath the degenerated retina, and the decrease was caused by a decrease in the luminal areas of the choroid. The authors concluded that the choroidal structures are differentially altered in eyes with RP. Whether these changes of the choroidal structures are associated with visual dysfunctions have not been determined.

We recently reported that the structural changes of the inner and outer subfoveal choroid are correlated with the disease activity in eyes with polypoidal choroidal vasculopathy and central serous chorioretinopathy.[16–18] In addition, we found that the effects of therapy for these diseases can be monitored by assessing the changes of the choroidal structures.[17,18] However, the structural changes of the inner and outer choroidal areas in eyes with RP have not been determined.

Thus, the purpose of this study was to quantify the luminal and stromal areas of the inner and outer subfoveal choroid in eyes with RP and compare them with the corresponding structures in control eyes. To accomplish this, the EDI-OCT images of the subfoveal choroid were binarized, and the sizes of the whole, luminal, and stromal areas of the inner and outer choroid were determined in eyes with RP and in normal control eyes. The correlations between the choroidal structures and visual functions were also determined.

Patients and Methods

This was a retrospective, observational case series of 100 eyes of 100 patients with typical RP and 60 eyes of 60 normal controls that were age-, sex-, and axial length–matched. All the patients diagnosed with typical RP at the Tokushima and Chiba University Hospitals and underwent spectral domain OCT, and retinal sensitivity measurements were included. Approval for the use of the procedures was obtained from the Institutional Review Boards of Tokushima and Chiba University Hospitals before the beginning of this study. All the patients gave their written informed consent to undergo the procedures before the measurements. The procedures conformed to the tenets of the Declaration of Helsinki.

The diagnosis of RP was based on the clinical history, fluorescein angiography, and full-field electroretinograms (ERGs) with the recording protocol conforming to the International Society for Clinical Electrophysiology of Vision standards. The ERGs of all the patients with RP were consistent with rod-cone dystrophy. Patients who were diagnosed with RP had the pathognomonic fundus changes such as attenuated retinal vessels, waxy atrophy of optic nerve head, and bone-spicule pigment clumping. Atypical RP cases such as sector RP and unilateral RP were excluded. Cases with retinal degenerative diseases that may specifically affect the choroid such as choroideremia, gyrate atrophy, or Bietti crystalline dystrophy were excluded. Patients with uveitis or any disease that could cause RP-like fundus changes were also excluded. Genetic testing was not performed for each case. Eyes with cataract, macular edema, epiretinal membrane, vitreomacular traction, myopic refractive error greater than −6.0 diopters, or other ocular diseases that might affect the clinical findings were also excluded. In patients who had two eyes that met the inclusion criteria, one eye was randomly chosen for the analyses. The demographic data and inheritance mode of the patients are presented in Table 1. There were no patients with X-linked RP.

All patients had standard ophthalmologic examinations including measurements of the best-corrected visual acuity (BCVA), axial length, and retinal sensitivity. Spectral domain OCT was performed on all the patients. Similar measurements were made on the control eyes, and all the examinations on an individual were performed on the same day. The BCVA was measured with a standard Japanese Landolt visual acuity chart, and the decimal BCVA was converted to the logarithm of the minimal angle of resolution (logMAR) units for the statistical analyses.

Spectral Domain Optical Coherence Tomography

Spectral domain OCT was performed with the Heidelberg Spectralis instrument (Heidelberg Engineering, Heidelberg, Germany) with the EDI-OCT format. The examinations were performed with the eye tracking system turned on, and 100 scans were

Table 1. Demographic Data of Patients With RP and Control Subjects

	Patients With RP (n = 100)	Normal Control (n = 60)	P
Age (years)	54.5 ± 14.5 (21–77)	55.3 ± 17.4 (21–73)	0.746
Sex	45 men/55 women	26 men/34 women	0.837
Axial length (mm)	23.21 ± 1.15 (21.10–25.96)	23.32 ± 0.72 (21.78–24.55)	0.521
BCVA (logMAR units) (Snellen ratios)	0.263 ± 0.478 (20/37) (−0.176 to 2.000 [CF - 20/12.5])	—	
Retinal sensitivity (mean deviation)	−14.83 ± 9.81 (−33.99 to 18.25)	—	
Foveal sensitivity (dB)	25.65 ± 9.40 (0–35.5)	—	
Width of EZ (μm)	2,478.5 ± 2,088.3 (0–8,112.5)	—	
CFT (μm)	207.2 ± 52.4 (69.7–290.3)	226.2 ± 15.9 (209.0–267.0)	**0.023**
Inheritance mode (n)			
AD	15		
AR	17		
Simplex	68		

A P value of <0.050 is considered statistically significant and is presented in bold.
AD, autosomal dominant; AR, autosomal recessive; CF, counting fingers.
Data are presented as mean ± SD (range).

averaged to improve the signal-to-noise ratio. The central foveal thickness (CFT), width of the ellipsoid zone (EZ), and central choroidal thickness (CCT) were measured manually with the caliper function embedded in the Spectralis instrument (Figure 1). All the EDI-OCT images were obtained between 11:00 and 13:00 hours to minimize the effect of the diurnal variations of the choroidal structures.[15]

*Quantification of Luminal, Stromal, and Overall Choroidal Areas by Binarization*

The binarization of the horizontal EDI-OCT images was performed by a modified Niblack method as described in detail (Figure 1).[14–18] The EDI-OCT images were analyzed using ImageJ software (ImageJ, version 1.47; NIH, Bethesda, MD). The examined choroidal area was 1,500-μm wide and centered on the fovea, and extended vertically from the Bruch membrane to the chorioscleral border.

Three choroidal vessels with lumens larger than 100 μm were randomly selected by the Oval Selection Tool on the ImageJ tool bar, and the average reflectivity of these three areas was calculated. This average reflectivity was set as the minimum value of the image reflectivity to minimize the noise in the EDI-OCT image. Then, the image was converted to an 8-bit image and adjusted by the Niblack Auto Local Threshold. The binarized image was converted to an RGB image again, and the luminal area was determined using the Threshold Tool on the RGB image. The light pixels were defined as the stromal areas and dark pixels as the luminal areas. After adding the data on the relationship between the distance on the fundus and the pixels in the EDI-OCT images, the luminal and stromal areas were automatically calculated.

Quantifications of the Inner and Outer Choroidal Areas

Quantifications of the inner and outer choroidal areas were performed on the binarized images.[16–18] The inner choroid included the choriocapillaris and medium choroidal vessel layer, and the outer choroid included the larger choroidal vessel layer. The border between the inner and outer choroid was determined by the methods proposed by Branchini et al[21] and Sim et al[22] with some modifications. The segmentation of the inner and outer choroidal areas was made on the binarized OCT images because the border was enhanced in the binarized images (Figure 1).[16–18] The inner/outer separation of the choroid was performed through the combined use of two methods for choroidal sublayer analysis.[21–23] Among the two methods, the inner/outer separation of the choroid was first performed based on the method of Branchini et al,[21] in which the choroidal sublayers were divided based on a cutoff diameter for large choroidal vessels. Branchini et al[21] conducted a pilot study measuring the diameter of the large choroidal vessels on the EDI-OCT images of healthy eyes. The mean diameter of healthy subjects was 100 μm (range 86–108 μm), which was then used as a cutoff for defining a large choroidal vessel for the choroidal vasculature analysis on EDI-OCT. The inner most points of several randomly selected large choroidal vessels of diameter more than 100 μm were plotted in the binarized EDI-OCT images, and lines of the inner/outer choroidal border were drawn by connecting these inner most points smoothly. If the choroidal vessels exhibiting the cutoff diameter were rarely observed, a method developed by Sim et al[22] was used as an alternative. In their study, the large choroidal vessel layer was defined as

Fig. 1. Representative EDI-OCT images and the converted binary images of one normal control eye and two RP eyes. Enhanced depth imaging OCT images were converted to binary images using ImageJ software. **A.** Enhanced depth imaging OCT image of the normal eye of a 68-year-old man. **B.** Enhanced depth imaging OCT image of the eye of a 40-year-old woman with RP and good visual function. Her BCVA was 20/16. The mean foveal sensitivity was 31.25 dB; width of the EZ was 3,346 μm, which extended beyond the area of the cropped image; and CFT was 220.59 μm. **C.** Enhanced depth imaging OCT image of the eye of a 46-year-old man with poor visual function. His BCVA was 20/50; mean foveal sensitivity was 19.75 dB; EZ width was 522 μm; and CFT was 116.10 μm. **A–C.** Red lines indicate the EZ width, and green double-headed arrows indicate the CFT in the images of eyes with RP. The dark areas are the luminal areas of the choroid and the light areas the stromal areas. The examined areas were set to be

1,500-μm wide in the subfoveal choroid. The irregular quadrilaterals surrounded by yellow lines were selected by the examiner. The images were adjusted by the Niblack Auto Local Threshold to obtain the binarized images. **D–F.** The binary images of the corresponding EDI-OCT images shown in **A–C.** The images show a relatively lower luminal/total choroidal area ratio for the inner choroid of the RP eye with poor visual function (**F**) than that of the normal eye and the RP eye with good visual function (**D** and **E**). The luminal areas were determined using the Threshold Tool. The light pixels were defined as the stromal choroid, and the dark pixels were defined as the luminal area. After adding the data of the distance between two adjacent pixels, the luminal and stromal areas were automatically calculated. Yellow lines indicate the margins of measured areas. Red dashed lines indicate the border between the inner and outer choroid.
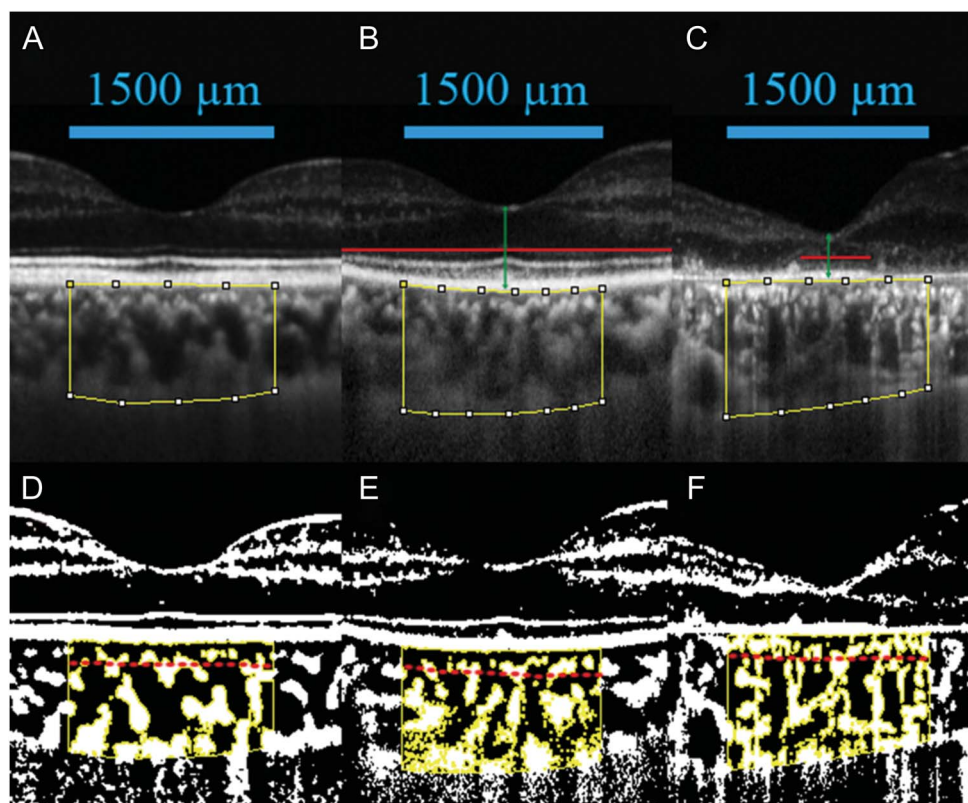
the outer choroid, consisting of large hyporeflective spaces representing large vascular luminal spaces. The medium choroidal vessel layer–choriocapillaris layer was defined as the inner choroid consisting of small- to medium-sized hyporeflective spaces, surrounded by hyperreflective stroma (increased scattering by high density of melanocytes), which gave this space a mottled appearance. Sim et al[22] reported that the thickness of the inner and outer choroidal sublayers can be quantified by this method with good reliability, repeatability, and reproducibility.

After measuring the luminal and stromal areas of the whole choroid, the examined 1,500-μm width region of interest was set to extend vertically from the Bruch membrane to the border of the inner and outer choroid to calculate the luminal and stromal areas of the inner choroid.[18] The values of the inner luminal and stromal areas were subtracted from those of the total luminal and stromal areas to obtain the outer luminal and stromal areas.

The binarization of the EDI-OCT image was performed three times for each image, and the values were averaged for the statistical analyses. Although the methods used for the analyses of the choroidal structures have been found to have high repeatability and reproducibility in normal and diseased eyes,[14–18] the intrarater correlation coefficient was calculated for the luminal and stromal areas of the inner and outer choroid for the 100 eyes with RP.

Retinal Sensitivity Measurements

The retinal sensitivity was measured with the Humphrey automated perimeter central 10-2 program with the FASTPAC strategy (Humphrey Field Analyzer; Carl Zeiss, San Leandro, CA) using stimulus size III and a background of 31.5 asb. The mean deviation of the static perimetric value was the sum of the sensitivity loss at all tested points. The foveal sensitivity was defined as the mean retinal sensitivity for the 4 stimulus locations covering the central 5°. The central 5° circle examined by the Humphrey automated perimeter is equivalent to a circle of approximate 1,500-μm diameter on the fundus of

an emmetropic eye examined in the binarized EDI-OCT image.[24]

Statistical Analyses

Unpaired *t*-tests were used to determine the significance of the differences between two independent groups. Pearson correlation tests were used to determine the significance of the correlations between the clinical findings and the EDI-OCT parameters. Partial correlation analyses were also used to examine the correlations between the clinical findings and EDI-OCT parameters adjusted for the axial length, age, and sex because these EDI-OCT parameters were reported to be significantly correlated with the axial length, age, and sex.[25] Analysis of covariance was used to examine the correlations between the inheritance mode and the EDI-OCT parameters adjusted for the axial length, age, and sex. The Bonferroni test was used for post hoc analysis. The intrarater correlation coefficients were calculated by a 1-way random effects model for measurements of agreement. A *P* value of <0.050 was considered statistically significant.

Results

The intrarater agreement was very high with all intraclass correlation coefficients >0.997 for the measurements of the luminal and stromal areas of the inner and outer choroid.

Comparisons of the Choroidal Structures Between Eyes With Retinitis Pigmentosa and Normal Controls

The whole and outer choroidal areas were significantly smaller in the eyes with RP than in the control eyes (both *P* < 0.001), but the inner choroidal area was not significantly different (*P* = 0.145, Table 2). In the inner choroid, the luminal area was significantly

smaller in the RP eyes than in the controls (*P* = 0.010), whereas the stromal area was not significantly different (*P* = 0.114; Figure 2 and Table 2). In the whole and outer choroid, the luminal and stromal areas were significantly smaller in the RP eyes (all *P* < 0.001, Table 2).

The ratio of luminal/total choroidal area (L/C ratio) of the whole and inner choroid was significantly smaller in the RP eyes than in the controls (*P* = 0.009, *P* < 0.001, respectively), but the L/C ratio of the outer choroid was not significantly different (*P* = 0.124, Figure 3). The CCT was significantly thinner in the RP eyes (*P* < 0.001, Table 2).

Correlation Between Choroidal Structures and Clinical Findings

Simple regression analysis showed that the L/C ratio of the inner choroid was significantly correlated with the BCVA, mean deviation, foveal sensitivity, width of the EZ, CFT, and CCT (all *P* < 0.050, Table 3 and Figure 4). The L/C ratio of the outer choroid was significantly correlated with the foveal sensitivity and CCT (*P* = 0.030, *P* < 0.001, respectively), but not with the BCVA, mean deviation, EZ width, and CFT (all *P* > 0.050). The L/C ratio of the whole choroid was significantly correlated with the BCVA, foveal sensitivity, CFT, and CCT (all *P* < 0.010), but not with the mean deviation and EZ width (all *P* > 0.100).

It has been reported that the choroidal structure was associated with the axial length, age, and sex.[25] Partial correlation analysis adjusted for the axial length, age, and sex showed that the L/C ratio of the inner choroid was significantly correlated with the BCVA, mean deviation, foveal sensitivity, EZ width, and CFT (all *P* < 0.005, Table 3), but not with the CCT (*P* = 0.614). The L/C ratio of the outer choroid was significantly correlated with the foveal sensitivity and CCT (*P* = 0.038, *P* < 0.001, respectively), but not with the

Table 2. Comparison of Choroidal Parameters in Patients With RP With Those of Normal Control

	Patients With RP (n = 100)	Normal Control (n = 60)	P
Whole choroidal area (mm²)	0.3396 ± 0.1222	0.4564 ± 0.1260	<**0.001**
Whole luminal area (mm²)	0.2250 ± 0.0893	0.3090 ± 0.0890	<**0.001**
Whole stromal area (mm²)	0.1146 ± 0.0378	0.1474 ± 0.0403	<**0.001**
Inner choroidal area (mm²)	0.0784 ± 0.0280	0.0841 ± 0.0128	0.145
Inner luminal area (mm²)	0.0544 ± 0.0232	0.0625 ± 0.0088	**0.010**
Inner stromal area (mm²)	0.0241 ± 0.0108	0.0216 ± 0.0069	0.114
Outer choroidal area (mm²)	0.2612 ± 0.1061	0.3723 ± 0.1176	<**0.001**
Outer luminal area (mm²)	0.1707 ± 0.0763	0.2464 ± 0.0833	<**0.001**
Outer stromal area (mm²)	0.0905 ± 0.0332	0.1258 ± 0.0378	<**0.001**
CCT (μm)	225.1 ± 83.0	304.7 ± 85.4	<**0.001**

A *P* value of <0.050 is considered statistically significant and is presented in bold.
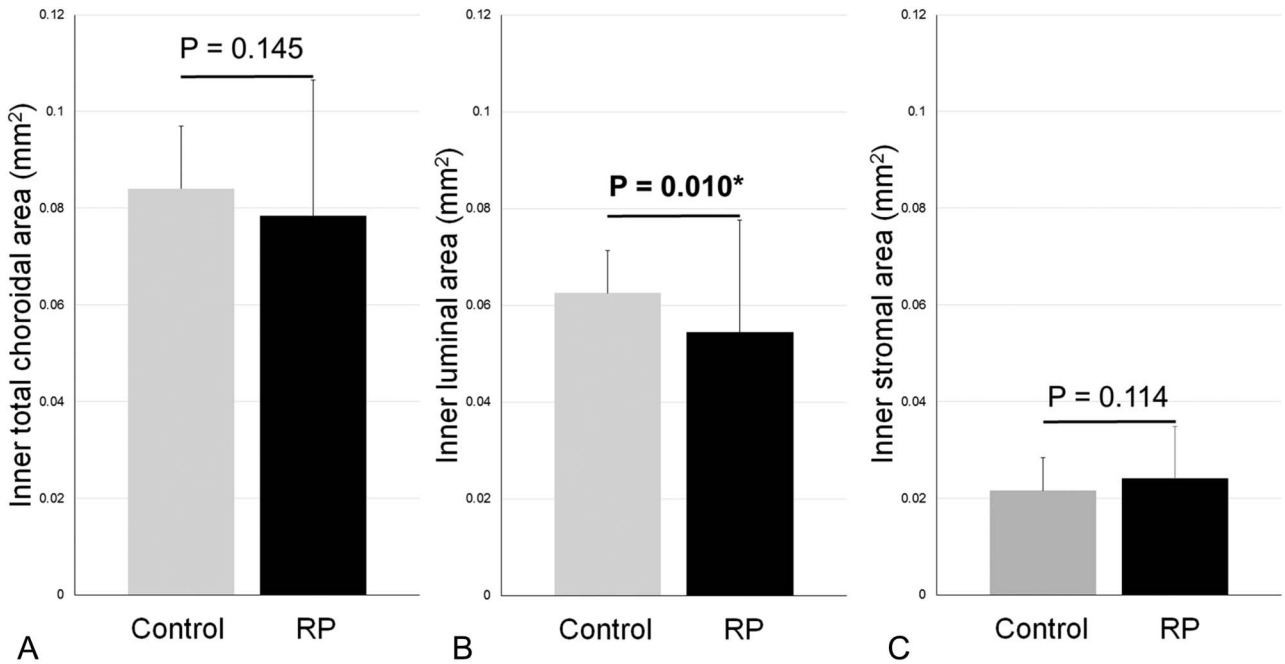
Fig. 2. Total choroidal, luminal, and stromal areas of the inner choroid in normal control eyes and eyes with RP. The inner luminal area is significantly smaller in eyes with RP than in controls (**B**), but the inner total choroidal and stromal areas are not significantly different (**A** and **C**). Bars indicate SDs. *$P < 0.050$.

BCVA, mean deviation, EZ width, and CFT (all $P > 0.100$). The L/C ratio of the whole choroid was significantly correlated with the BCVA, mean deviation, foveal sensitivity, CFT, and CCT (all $P < 0.050$), but not with the EZ width ($P = 0.050$).

The CCT was not significantly correlated with the BCVA, mean deviation, foveal sensitivity, and CFT (r = −0.040, $P = 0.692$; r = −0.134, $P = 0.184$; r = 0.041, $P = 0.689$; and r = −0.168, $P = 0.096$, respectively) using simple regression analysis. There
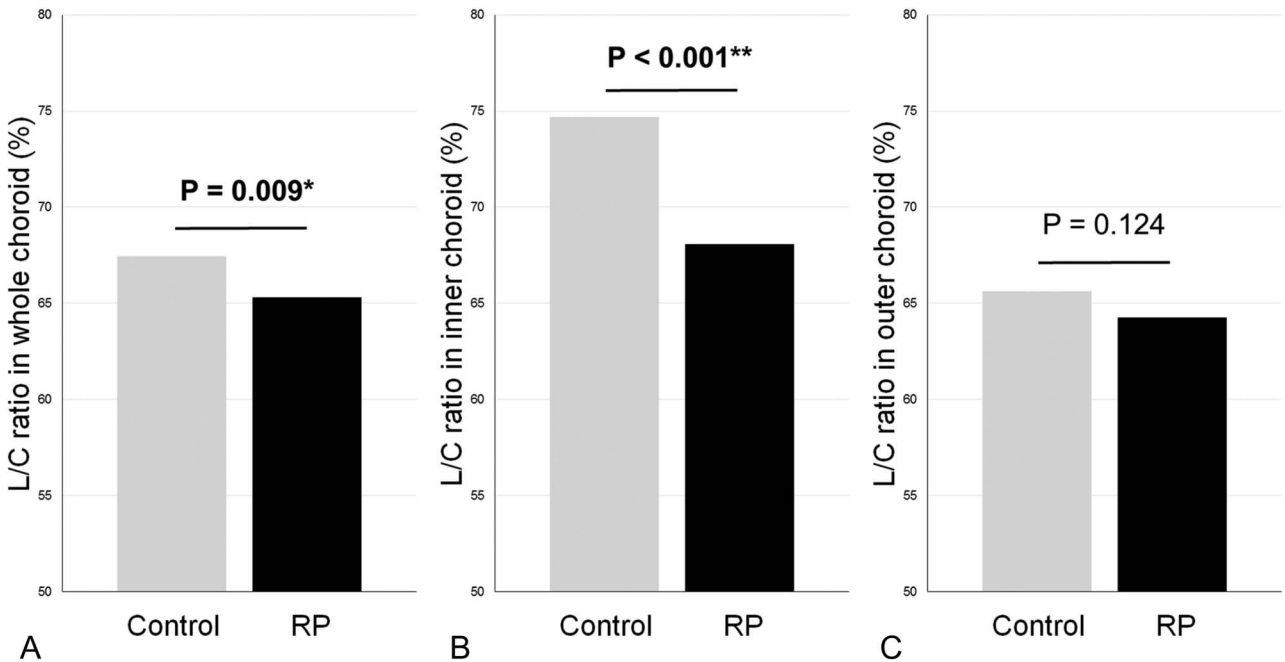

Fig. 3. Ratio of luminal area to the total choroidal area (L/C ratio) of the whole, inner, and outer choroid in normal control eyes and eyes with RP. The L/C ratio in the whole and inner choroid is significantly lower in eyes with RP than in controls (**A** and **B**), but the L/C ratio in the outer choroid is not significantly different (**C**). *$P < 0.010$ and **$P < 0.001$.

Table 3. Correlation Between Choroidal Parameters and Visual Functions or Retinal Parameters

	L/C Ratio of the Whole Choroid (%)	L/C Ratio of the Inner Choroid (%)	L/C Ratio of the Outer Choroid (%)
Simple regression analysis			
BCVA (logMAR units)	**r = −0.419**	**r = −0.500**	r = −0.181
	P < 0.001	**P < 0.001**	P = 0.072
Retinal sensitivity (mean deviation)	r = 0.152	**r = 0.266**	r = −0.004
	P = 0.132	**P = 0.007**	P = 0.971
Foveal sensitivity (dB)	**r = 0.426**	**r = 0.480**	**r = 0.218**
	P < 0.001	**P < 0.001**	**P = 0.030**
Width of EZ (μm)	r = 0.092	**r = 0.241**	r = −0.078
	P = 0.362	**P = 0.016**	P = 0.438
CFT (μm)	**r = 0.282**	**r = 0.396**	r = 0.108
	P = 0.005	**P < 0.001**	P = 0.285
CCT (μm)	**r = 0.402**	**r = 0.207**	**r = 0.451**
	P < 0.001	**P = 0.039**	**P < 0.001**
Partial correlation analysis (adjusted by axial length, age, and sex)			
BCVA (logMAR units)	**r_p = −0.399**	**r_p = −0.481**	r_p = −0.153
	P < 0.001	**P < 0.001**	P = 0.136
Retinal sensitivity (mean deviation)	**r_p = 0.249**	**r_p = 0.345**	r_p = 0.056
	P = 0.014	**P = 0.001**	P = 0.587
Foveal sensitivity (dB)	**r = 0.434**	**r_p = 0.481**	**r = 0.212**
	P < 0.001	**P < 0.001**	**P = 0.038**
Width of EZ (μm)	r_p = 0.200	**r_p = 0.332**	r_p = −0.011
	P = 0.050	**P = 0.001**	P = 0.912
CFT (μm)	**r_p = 0.353**	**r_p = 0.452**	r_p = 0.153
	P < 0.001	**P < 0.001**	P = 0.135
CCT (μm)	**r_p = 0.241**	r_p = 0.052	**r = 0.355**
	P = 0.017	P = 0.614	**P < 0.001**

A P value of <0.050 is considered statistically significant and is presented in bold.
L/C ratio, ratio of luminal/total choroidal area; r_p, partial correlation coefficient.

was a significant correlation between the CCT and EZ width (r = −0.197, P = 0.049), but this was not relevant (|r| < 0.2).

To determine the correlation between the inheritance mode and the choroidal structure, analysis of covariance was performed with adjustments made for the axial length, age, and sex. The results showed that the L/C ratio of the inner and whole choroid was significantly different among the autosomal dominant, autosomal recessive, and simplex RP (P = 0.010, P = 0.016, respectively; Table 4). The L/C ratio of the inner and whole choroid was lowest in eyes with autosomal recessive RP.

Discussion

The results of earlier studies indicated that the subfoveal choroid was significantly thinner in eyes with RP.[12,13] Our results showed that the L/C ratio of the inner and whole choroid was significantly lower in eyes with RP than those of the controls. However, the L/C ratio of the outer choroid was not significantly different from that of the controls. These results

suggest that the choroidal thinning in RP eyes is caused mainly by a decrease of the luminal areas, and the structural changes are different between the inner and outer choroid. A decrease in the choroidal blood flow has also been reported in patients with RP.[3–5] The results of this study indicate that the luminal area of the inner choroid was significantly smaller in eyes with RP than in controls, but the stromal area was not significantly different. These results suggest a constriction or obliteration of the inner choroidal vessels. In the RP eyes, the inner choroidal L/C ratio was significantly correlated with the BCVA, mean deviation, foveal sensitivity, EZ width, and CFT after adjusting for the axial length, age, and sex. These results indicate that the choroidal structure is altered in association with the progression of the RP disease process because these visual and retinal parameters can accurately reflect the disease progression.[26]

Kawano et al[20] have shown that there was a significant correlation between the changes in the choroidal structures and the presence of the degenerated retina in eyes with RP. They reported that the overall cross-sectional choroidal area in the EDI-OCT images in
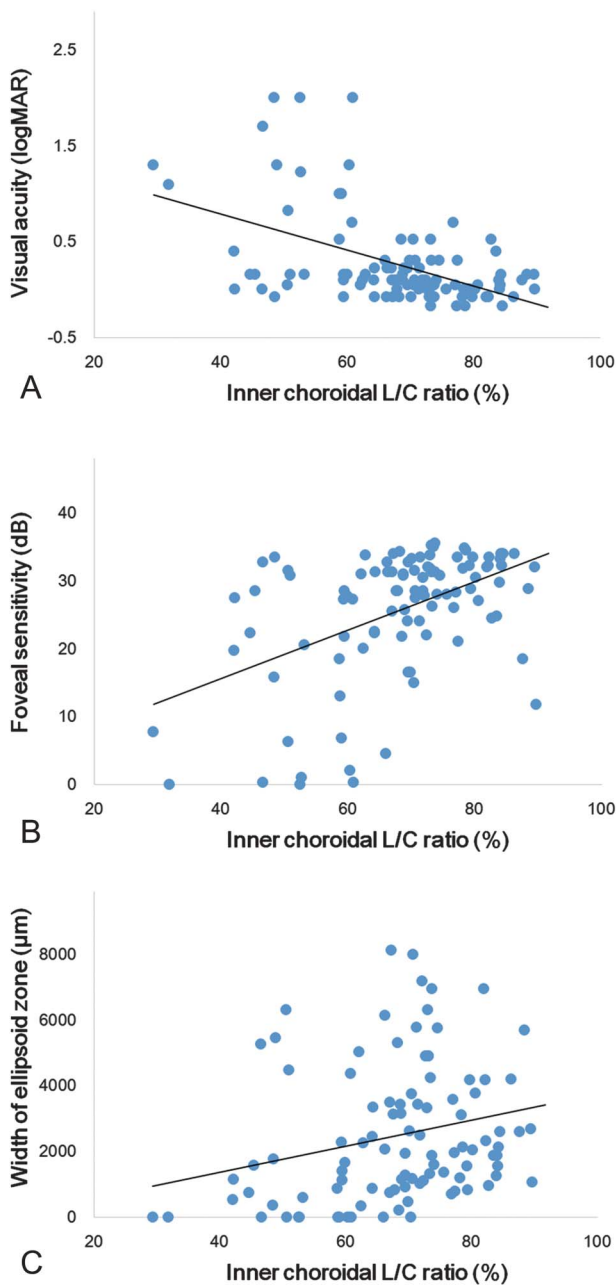
Fig. 4. Correlations between the ratio of the luminal/total choroidal area (L/C ratio) of the inner choroid and visual function or central retinal structure in eyes with RP. **A.** Simple regression analysis shows that the L/C ratio of the inner choroid is significantly correlated with the visual acuity in logMAR units (r = −0.500, $P < 0.001$). The solid line represents the linear regression line, y = −0.019x + 1.542. **B.** The L/C ratio of the inner choroid is significantly correlated with the foveal sensitivity (r = 0.480, $P < 0.001$). The foveal sensitivity is defined as the mean sensitivity of the 4 stimulus locations in the central 5° of the visual fields of the Humphrey automated perimeter. The solid line represents the linear regression line, y = 0.358x + 1.242. **C.** The L/C ratio of the inner choroid is significantly correlated with the width of EZ (r = 0.241, P = 0.016). The solid line represents the linear regression line, y = 39.647x − 220.2.

eyes with RP was significantly smaller than that in normal eyes. The luminal area was significantly smaller in RP eyes than in control eyes. The L/C ratio of the whole choroid was significantly smaller in the RP eyes, which was consistent with our results. Kawano et al[20] also reported that the L/C ratio was significantly smaller in the nasal and temporal areas that have more retinal degeneration in RP eyes than in the corresponding areas of the control eyes. In eyes with RP, the L/C ratio was significantly smaller in the area with greater retinal degeneration than in that with less retinal degeneration. These results suggest that the alterations of the choroidal structure in eyes with RP are related to the degeneration of the retina.

The results of a histological study showed that there was a reduction in the number of choroidal capillaries and the presence of structural damage of the choriocapillaris in the eyes of animal models of RP[8,9] and in eyes of humans with RP.[1,27] The choriocapillaris was invariably missing from the retinal regions that had lost photoreceptors and had bone-spicule pigmentation. Because of the close interdependence of the choriocapillaris, retinal pigment epithelium (RPE), and photoreceptors, it is not clear whether the loss of the capillary bed is secondary to the death of the photoreceptors or to the loss of the neighboring RPE cells. However, it has been reported that the loss of the RPE in previously healthy rabbit eyes leads to secondary atrophy of the choriocapillaris.[28] Another study on porcine retinas reported that the choriocapillaris becomes atrophic within 1 week after a debridement of the RPE.[29] These results suggest that the loss of RPE cells can lead to alterations of the choriocapillaris. However, it is difficult to determine the actual changes in the choroidal vascular components by histological studies because the vascular appearance can be altered during the histological preparations.[20] Kawano et al[20] have provided strong evidence that the luminal areas were smaller in the more degenerated areas of the retina in RP eyes in the EDI-OCT images. In addition, our results showed that the decrease in the L/C ratio was more prominent in the inner choroid where the choriocapillaris exists than in the outer choroid.

In patients with RP at a relatively advanced stage, the ocular pulse amplitude, an indirect measure of pulsatile choroidal perfusion, was found to be reduced significantly.[3,4] The decrease of the inner choroidal luminal area in this study may be a manifestation of this decreased choroidal flow. Falsini et al[5] used confocal laser Doppler flowmetry and focal macular ERGs to determine whether functional macular changes were associated with corresponding deficits in the subfoveal superficial choroid circulation in eyes with RP. The signals of the laser Doppler

Table 4. Correlation Between Inheritance Mode and Choroidal Parameters (Adjusted by Axial Length, Age, and Sex)

	Inheritance Mode				P (Bonferroni Test)		
	AD	AR	Sim	P (for All Groups)	AD vs. AR	AD vs. Sim	AR vs. Sim
L/C ratio of the whole choroid (%)	63.60 ± 1.36	62.63 ± 1.26	66.35 ± 0.63	**0.016**	>0.999	0.215	**0.030**
L/C ratio of the inner choroid (%)	64.15 ± 3.13	61.38 ± 2.90	70.61 ± 1.45	**0.010**	>0.999	0.199	**0.017**
L/C ratio of the outer choroid (%)	64.09 ± 1.54	62.80 ± 1.43	64.65 ± 0.71	0.514	>0.999	>0.999	0.754
CCT (μm)	227.1 ± 17.4	206.1 ± 16.1	229.4 ± 8.1	0.437	>0.999	>0.999	0.607

A P value of <0.050 is considered statistically significant and is presented in bold.
AD, autosomal dominant; AR, autosomal recessive; L/C ratio, ratio of luminal/total choroidal area; Sim, simplex.
Data are presented as estimated marginal mean ± SE.

flowmetry in the subfoveal choroid originate predominantly from the choriocapillaris. They reported that the choroidal blood flow and velocity were significantly reduced in the patients with RP compared to controls. In patients with RP, the choroidal blood flow and velocity were significantly correlated with prolongations of the implicit times of the ERGs, and the choroidal blood volume was significantly correlated with the ERG amplitudes. In addition, the choroidal blood volume and flow tended to be more reduced in RP patients with more advanced Goldmann visual field loss compared with those with relatively preserved visual fields. These findings suggested that there is a significant association between the abnormal circulation in the superficial layers of the choroid and the RP-associated central cone-mediated dysfunctions. Falsini et al[5] suggested that alterations of the choroidal circulation may either be associated with the disease or play a role in its pathogenesis or both. Consistent with these findings, the results of our study suggested a close relationship between the inner choroidal structure and the central visual functions and central retinal structures.

In eyes with RP, the rod photoreceptors are the primary tissues that degenerate.[1] After the rod photoreceptors degenerate, the inner retinal neurons and RPE also degenerate. The results of the study by Kawano et al[20] and our study indicate that the luminal area of the choroid was smaller in the RP eyes. The decrease in the choroidal luminal area indicates that the number and/or diameter of vessels has decreased. Vascular endothelial growth factor (VEGF) has a vasodilatory effect by upregulating the endothelial nitric oxide synthase–dependent pathways, and thus, a VEGF downregulation can lead to the vascular contraction.[20] Vascular endothelial growth factor plays an important role in maintaining the choroidal homeostasis and is secreted mainly on the choroidal side of the RPE.[30] The RPE degeneration observed in eyes with RP may cause a decrease of the VEGF secretion from RPE cells resulting in vascular contraction and a decrease of the luminal area of the choroid in the EDI-OCT images. In fact, Kurihara et al[31] reported that a conditional knock out of VEGF-A in adult mouse RPE cells leads to a rapid loss of vision and choriocapillaris. This VEGF-A knock out mice also had a rapid dysfunction of the cone photoreceptors. However, the rod photoreceptor function was not sensitive to the VEGF-A inactivation. The authors concluded that the RPE-derived VEGF is required for maintenance of the choriocapillaris and for the cone photoreceptors, and that the rod photoreceptors may be supported by a minimal vasculature not dependent on RPE-derived VEGF for survival.

Taken together, we suggest that the RPE degeneration observed in eyes with RP leads to a decrease of the RPE-derived VEGF, damage of the choriocapillaris, and eventual dysfunction of cone photoreceptors. Our results of the close relationship between the inner choroidal structure and the central visual functions and central retinal structure support this suggestion.

The CCT was not significantly correlated with the BCVA, mean deviation, foveal sensitivity, and CFT. A previous study also reported that the correlation between the subfoveal choroidal thickness and visual acuity was not significant in patients with RP.[32] These results suggest that the CCT is not associated with the visual acuity in eyes with RP, which supports the usefulness of choroidal analyses using the binarization of the EDI-OCT images.

Most recently, Murakami et al[33] reported on the relationships among the foveal blood flow, choroidal structure in binarized EDI-OCT images, and central visual function in 52 patients with RP. Their results showed that the L/C ratio of the whole choroid was not significantly correlated with the central visual function such as BCVA, foveal sensitivity, mean deviation, and EZ width. Our results showed that the inner choroidal L/C ratio, rather than the whole choroidal L/C ratio, was significantly correlated with the central visual functions in 100 RP eyes. The reason for this discrepancy may be related to the smaller sample size in their study. In addition, the macular area was not impaired in most of their patients with RP (mean BCVA was 20/23 in their study and 20/37 in this study), and these subjects were not appropriate for analyzing the changes of the submacular choroidal structure in eyes of patients with RP. In fact, Kawano et al[20] reported that the choroidal structure was not different in unaffected macular area between RP and healthy eyes. In addition, analysis of choroidal inner/outer layer was not performed in the study of Murakami et al.[33]

It has been reported that the autosomal recessive form of RP is generally characterized by the earlier onset, more rapid progression of the visual deterioration, and increased risk of total blindness in adult life.[34] Consistent with these findings, the L/C ratio of the inner and whole choroid was lowest in eyes with autosomal recessive RP in this study.

Several studies have been reported on the accuracy of the inner/outer separation of the choroid in eyes with retinal degeneration. Hirashima et al[35] investigated the inner and outer choroidal thickness in Bietti crystalline dystrophy and RP, and they reported that the intraclass correlation coefficient values of the subfoveal inner choroidal thickness measurements were 0.964 and that interinvestigator reliability of the measurements was very good. Adhi et al[36] examined the inner and outer choroidal thickness in Stargardt disease and reported that the intraclass correlation coefficients for subfoveal outer choroidal thickness measurements between 2 observers were 0.94 for healthy eyes and 0.90 in eyes with Stargardt disease. The intraclass correlation coefficients for eyes with Stargardt disease were slightly worse than those for healthy eyes but were still good enough for analyses of the choroidal structure. Adhi et al[13] also examined the inner and outer choroidal thickness in eyes with RP, and the large choroidal vessel layer could be delineated with a strong interobserver agreement.

This study has limitations. First, this was a retrospective study that can have sampling biases. Second, the manual segmentation of the inner and outer choroid was not completely objective.[18] Third, genetic testing was not performed. Finally, this study is a cross-sectional study, and a prospective longitudinal study of the choroidal structure in patients with RP will help shed further light on the role of the choroid in the pathogenic changes in RP eyes.

In conclusion, binarization of the EDI-OCT images is a useful and noninvasive method to quantify the choroidal structures in patients with RP. Our results provide in situ evidence for a decrease of the inner choroidal luminal areas and significant correlations between the inner choroidal structure and the central visual functions and retinal structures in RP eyes.

Acknowledgments

References

1. Milam AH, Li ZY, Fariss RN. Histopathology of the human retina in retinitis pigmentosa. Prog Retin Eye Res 1998;17:175–205.
2. Léveillard T, Mohand-Saïd S, Lorentz O, et al. Identification and characterization of rod-derived cone viability factor. Nat Genet 2004;36:755–759.
3. Langham ME, Kramer T. Decreased choroidal blood flow associated with retinitis pigmentosa. Eye 1990;4:374–381.
4. Schmidt KG, Pillunat LE, Kohler K, Flammer J. Ocular pulse amplitude is reduced in patients with advanced retinitis pigmentosa. Br J Ophthalmol 2001;85:678–682.
5. Falsini B, Anselmi GM, Marangoni D, et al. Subfoveal choroidal blood flow and central retinal function in retinitis pigmentosa. Invest Ophthalmol Vis Sci 2011;52:1064–1069.

6. Tanito M, Kaidzu S, Anderson RE. Delayed loss of cone and remaining rod photoreceptor cells due to impairment of choroidal circulation after acute light exposure in rats. Invest Ophthalmol Vis Sci 2007;48:1864–1872.

7. Cellini M, Strobbe E, Gizzi C, et al. ET-1 plasma levels and ocular blood flow in retinitis pigmentosa. Can J Physiol Pharmacol 2010;88:630–635.

8. May CA, Narfström K. Choroidal microcirculation in Abyssinian cats with hereditary rod-cone degeneration. Exp Eye Res 2008;86:537–540.

9. May CA, Horneber M, Lütjen-Drecoll E. Quantitative and morphological changes of the choroid vasculature in RCS rats and their congenic controls. Exp Eye Res 1996;63:75–84.

10. Krill AE, Archer D, Newell FW. Fluorescein angiography in retinitis pigmentosa. Am J Ophthalmol 1970;69:826–835.

11. Yamamoto S, Sugawara T, Murakami A, et al. Topical isopropyl unoprostone for retinitis pigmentosa: microperimetric results of the phase 2 clinical study. Ophthalmol Ther 2012; 1:5.

12. Ayton LN, Guymer RH, Luu CD. Choroidal thickness profiles in retinitis pigmentosa. Clin Exp Ophthalmol 2013;41:396–403.

13. Adhi M, Regatieri CV, Branchini LA, et al. Analysis of the morphology and vascular layers of the choroid in retinitis pigmentosa using spectral-domain OCT. Ophthalmic Surg Lasers Imaging Retina 2013;44:252–259.

14. Sonoda S, Sakamoto T, Yamashita T, et al. Choroidal structure in normal eyes and after photodynamic therapy determined by binarization of optical coherence tomographic images. Invest Ophthalmol Vis Sci 2014;55:3893–3899.

15. Kinoshita T, Mitamura Y, Shinomiya K, et al. Diurnal variations in luminal and stromal areas of choroid in normal eyes. Br J Ophthalmol 2017;101:360–364.

16. Sonoda S, Sakamoto T, Kuroiwa N, et al. Structural changes of inner and outer choroid in central serous chorioretinopathy determined by optical coherence tomography. PLoS One 2016;11:e0157190.

17. Kinoshita T, Mitamura Y, Mori T, et al. Changes in choroidal structures in eyes with chronic central serous chorioretinopathy after half-dose photodynamic therapy. PLoS One 2016;11: e0163104.

18. Daizumoto E, Mitamura Y, Sano H, et al. Changes of choroidal structure after intravitreal aflibercept therapy for polypoidal choroidal vasculopathy. Br J Ophthalmol 2017;101:56–61.

19. Agrawal R, Gupta P, Tan KA, et al. Choroidal vascularity index as a measure of vascular status of the choroid: measurements in healthy eyes from a population-based study. Sci Rep 2016;6:21090.

20. Kawano H, Sonoda S, Saito S, et al. Choroidal structure altered by degeneration of retina in eyes with retinitis pigmentosa. Retina 2017;37:2175–2182.

21. Branchini LA, Adhi M, Regatieri CV, et al. Analysis of choroidal morphologic features and vasculature in healthy eyes using spectral-domain optical coherence tomography. Ophthalmology 2013;120:1901–1908.

22. Sim DA, Keane PA, Mehta H, et al. Repeatability and reproducibility of choroidal vessel layer measurements in diabetic retinopathy using enhanced depth optical coherence tomography. Invest Ophthalmol Vis Sci 2013;54:2893–2901.

23. Park KA, Oh SY. An optical coherence tomography-based analysis of choroidal morphologic features and choroidal vascular diameter in children and adults. Am J Ophthalmol 2014; 158:716–723.

24. Suzuki T, Terasaki H, Niwa T, et al. Optical coherence tomography and focal macular electroretinogram in eyes with epiretinal membrane and macular pseudohole. Am J Ophthalmol 2003;136:62–67.

25. Sonoda S, Sakamoto T, Yamashita T, et al. Luminal and stromal areas of choroid determined by binarization method of optical coherence tomographic images. Am J Ophthalmol 2015;159:1123–1131.

26. Aizawa S, Mitamura Y, Hagiwara A, et al. Changes of fundus autofluorescence, photoreceptor inner and outer segment junction line, and visual function in patients with retinitis pigmentosa. Clin Exp Ophthalmol 2010;38:597–604.

27. Li ZY, Possin DE, Milam AH. Histopathology of bone spicule pigmentation in retinitis pigmentosa. Ophthalmology 1995; 102:805–816.

28. Korte GE, Reppucci V, Henkind P. RPE destruction causes choriocapillary atrophy. Invest Ophthalmol Vis Sci 1984;25: 1135–1145.

29. Del Priore LV, Kaplan HJ, Hornbeck R, et al. Retinal pigment epithelial debridement as a model for the pathogenesis and treatment of macular degeneration. Am J Ophthalmol 1996; 122:629–643.

30. Saint-Geniez M, Kurihara T, Sekiyama E, et al. An essential role for RPE-derived soluble VEGF in the maintenance of the choriocapillaris. Proc Natl Acad Sci U S A 2009;106:18751–18756.

31. Kurihara T, Westenskow PD, Bravo S, et al. Targeted deletion of VEGFa in adult mice induces vision loss. J Clin Invest 2012;122:4213–4217.

32. Dhoot DS, Huo S, Yuan A, et al. Evaluation of choroidal thickness in retinitis pigmentosa using enhanced depth imaging optical coherence tomography. Br J Ophthalmol 2013;97:66–69.

33. Murakami Y, Funatsu J, Nakatake S, et al. Relations among foveal blood flow, retinal-choroidal structure, and visual function in retinitis pigmentosa. Invest Ophthalmol Vis Sci 2018; 59:1134–1143.

34. Merin S, Auerbach E. Retinitis pigmentosa. Surv Ophthalmol 1976;20:303–346.

35. Hirashima T, Miyata M, Ishihara K, et al. Choroidal vasculature in Bietti crystalline dystrophy with CYP4V2 mutations and in retinitis pigmentosa with EYS mutations. Invest Ophthalmol Vis Sci 2017;58:3871–3878.

36. Adhi M, Read SP, Ferrara D, et al. Morphology and vascular layers of the choroid in Stargardt disease analyzed using spectral-domain optical coherence tomography. Am J Ophthalmol 2015;160:1276–1284.